RESEARCH ARTICLE                                                          OPEN ACCESS

# Mathematical modeling and experimental study of a modified hemispherical solar still

R. Fallahzadeh[a], N. Gholamiarjenaki[b], Z. Nonejad[b], M. Fallahzadeh[c], M. Saghi[a]

[a] *Chemical Engineering Department, Faculty of Engineering, Ferdowsi University of Mashhad, Mashhad, Iran*
[b] *Chemical Engineering Department, Faculty of Engineering, University of Isfahan, Isfahan, Iran*
[c] *Computer Engineering Department, Faculty of Engineering, Islamic Azad University, Science and Research Tehran (Yazd), Yazd, Iran*
*Corresponding Author; R. Fallahzadeh*

**A B S T R A C T**
Due to the concerning reduction in freshwater resources in many parts of the world and necessity of using saline water, the solar distillers have gained importance considering solar energy as a clean and cost-effective resource. In this study, the performance of a modified simple hemispherical solar still was theoretically and experimentally assessed under the outdoor conditions of Mashhad, Iran (latitude of $36^0 18'$ ; longitude of $59^0 34'$ ). After performing several experimental tests, the daily distilled water output from the still was observed to range between 2.72 and 3.17 Lit/day. Comparing experimental results with the results obtained by modeling of the still, it was revealed that Clark's model, among all the common thermal models to predict the performance of solar stills, was more consistent with experimental data. Furthermore, the modeling results indicated that the efficiency of the still was enhanced by more than 1% by decreasing the thickness of the glass cover. Moreover, thermal conductivity and thickness of insulation played a key role in the efficiency of the still so that the efficiency can be augmented to 60% by decreasing and increasing the thermal conductivity and thickness of insulation, respectively.
**Keywords:** hemispherical solar still; mathematical modeling; experimental study; glass cover thickness; insulation

-----------------------------------------------------------------------------------------------------------------------------
-----------------------------------------------------------------------------------------------------------------------------

## I.    INTRODUCTION

The demand for drinking water is increasing due to the swift growth of population and high pollution of current resources [1]. One solution to tackle the problem of water shortage is to use desalination systems that benefit from renewable energy resources such as solar energy. A solar still is a very simple method for water distilling that exploits solar energy and, in turn, can be immensely applicable in tropical areas such as the Middle East. Employing solar stills as an easy and cheap approach for desalination traced back to the 16th century [2], though a significant application of solar distillation was not reported from the 16th to 19th centuries [3]. The first common solar still plant was built by the Swedish engineer Charles Wilsonin 1872 [4]. From that time on, many stills have been build base on the very primary principles, although numerous changes have been made in geometry, materials, manufacture methods, and operation. The efficiency of solar stills depends on various factors including the design of the still [5]. To improve the performance of solar stills, different unconventional shapes have been proposed, namely

spherical stills [6-7], triangular stills [8-13], and tubular stills [14-18]. Also, hemispherical stills are included in the modern designs of stills that have been rarely investigated. They are designed and manufactured to increase the absorbed solar energy and have outperformed a standard-single-slope single-basin solar still as well.

After fabricating a hemispherical solar still and conducting an experimental study on it, Ismaill [19] observed that an increase in the water depth by 50% caused a reduction in the efficiency by 8%. Furthermore, Arunkumar et al. [20] carried out an experimental study on the effect of water flow over the cover surface on a hemispherical solar still. The obtained results indicated the efficiency increase by 42% once applying water flow. By an experimental investigation along with the simulation of a hemispherical solar still by the aid of ANSYS CFS, Panchal et al. [21] showed that the simulation results agreed well with the results of experimental work for the prediction of solar still performance.It was intended to enhance the collector efficiency as much as possible in this study by changing the basin shape from conical to cylindrical (low height) and also considering a glass cover surface with the slope equal to the

latitude of the experiment site.Generally, since experimental studies are highly expensive and time-consuming, mathematical modeling can be the best alternative to reach well-suited designs and operational parameters for solar stills [22]. Accordingly, many of the parameters affecting the production of solar stills have been investigated through modeling.However, since most modeling efforts have neglected temperature gradient in glass cover, the effect of glass cover thickness on the efficiency of stills have not been addressed with the association of modeling.The present study aims at investigating the effect of glass cover thickness on the solar still productivity by assuming the glass cover as two discrete internal and external parts.Furthermore, the efficiency change due to the variations of insulation thickness and conductivity is evaluated.

## II. EXPERIMENTAL SETUP AND PROCEDURE

A schematic view of the solar still setup and image of the fabricated still are shown in Figs. 1 and 2, respectively. The solar still comprises mild steel circular basin carrying saline water with the diameter of 0.4m, the height of 0.15m, and thickness of 0.003m (operating as the basin). The basin was painted black to increase absorptivity. The still was filled with saline water to the height of 0.08m. The sides and bottom of the solar still were covered with polyurethane foam (PUF) insulation with the thickness of 0.05m. As shown in Fig. 1, a tube was mounted on the sidewall to be used as the inlet port of saltwater. The incident solar radiation passes through a glass cover with the thickness of 0.003m —mounted on the top of the solar still— and heat is then absorbed by the black plate. The water of the basin is heated by the solar radiation and evaporation occurs. The formed vapor is condensed on the internal surface of the glass cover which has lower temperature due to its contact with ambient air. The condensate water is then flowed out towards a galvanized steel gutter connected to the outlet port. The distillate output from the still is collected and measured by a plastic container (with the capacity of 500ml and accuracy of 5ml) located beneath the outlet port.
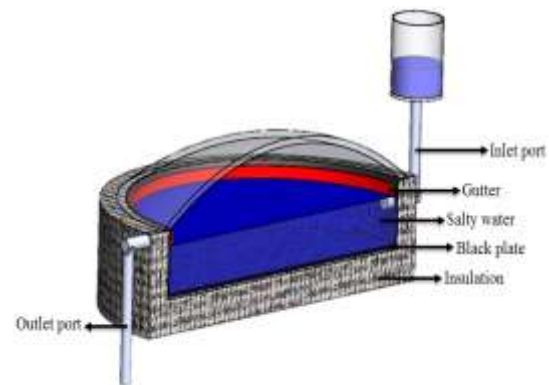


**Fig. 1.** Cross-sectional view of the hemispherical solar still



**Fig. 2.** A photograph of the fabricated hemispherical solar still

Experimental tests were performed in Mashhad, Iran (latitude of $36^0 18'$; longitude of $59^0 34'$). To absorb the maximum annual solar radiation, the surface of glass cover was considered with the slope approximately equal to the latitude (35°) relative to the horizontal axis. Before the initiation of each experiment, dust was removed from the surface of the glass cover and the basin was filled with saline water through the inlet port. Experiments started around 7:00 am to 6:00 pm, while the still was placed outside subjected to sunshine for about one hour before the experiments. Experiments were performed on three different days in a week in a typical summer month, June 2019. Experimental data were recorded per hour.

The wind speed and ambient temperature were measured by digital wind anemometer with the velocity range of 0-30 m/s and accuracy of ±0.1 m/sand the temperature range of -10 –45 centigrade and accuracy of ± 0.2 centigrade. The intensity of solar radiation was measured by a solarimeter (with

the range of 0–1200 W/m$^2$ and accuracy of ±5 W/m$^2$).

## III. MATHEMATICAL MODELING

The Transient modeling of the solar still with the aid of energy balance over its different parts was performed by MATLAB software. To simplify the modeling process, the following assumptions were made:

1) The variation rate at the temperatures of different parts of the system is so slight that the system always remains in the steady-state condition.

2) There is no vapor leakage in the still.

3) There is no temperature gradient in water depth, basin, and insulation.

4) Reduction in the basin water due to evaporation can be neglected in comparison to the total water inside the still.

5) The areas of water surface, glass cover, and basin are equal.

6) Since the inclination of the glass cover with the horizontal axis is small, its effect can be neglected.

As per the above assumptions, the energy balance equations for the main parts of the system are expressed as follows:

### 3.1. Heat balance equation for the glass cover outer surface

$$\frac{K_g}{L_g}\left(T_{gi} - T_{go}\right) = h_{t,go-a}\left(T_{go} - T_a\right) \qquad (1)$$

stands for total top heat loss coefficient between glass cover outer surface and atmosphere. Also, since heat loss from the top of the glass cover to the environment consists of convection (to ambient air) and radiation (to the sky), is the sum of convective heat transfer coefficient from the glass cover outer surface to ambient ( ) and radiative heat transfer coefficient from the glass cover outer surface to ambient ( ) and thus:

$$h_{t,go-a} = h_{c,go-a} + h_{r,go-a} \qquad (2)$$

The convective heat transfer coefficient from the top part of the glass can be calculated as given below [23]:

$$h_{c,go-a} = 2.8 + 3V \qquad (3)$$

And radiative heat transfer coefficient loss from the top can be referenced to the sky and computed from:

$$h_{r,go-a} = \varepsilon_g \sigma\left[\frac{\left(T_{go} + 273.15\right)^4 - \left(T_{sky} + 273.15\right)^4}{T_{go} - T_a}\right] \qquad (4)$$

represents the sky temperature and is calculated by the following relation using ambient temperature [24]:

$$T_{sky} = 0.0552T_a^{1.5} \qquad (5)$$

### 3.2. Heat balance equation for the glass cover inner surface

$$\left(1 - \rho_g\right)\alpha_g G + h_{t,w-gi}\left(T_w - T_{gi}\right) = \frac{K_g}{L_g}\left(T_{gi} - T_{go}\right) \qquad (6)$$

stands for the total heat transfer coefficient from water to glass cover inner surface and is the sum of convective heat transfer coefficient ( ), evaporative heat transfer coefficient from water to glass cover ( ), and radiative heat transfer coefficient from water to glass cover ( ):

$$h_{t,w-gi} = h_{c,w-gi} + h_{e,w-gi} + h_{r,w-gi} \qquad (7)$$

Can be obtained from the following relation:

$$h_{r,w-gi} = \varepsilon_{eff}\sigma\left[\left(T_w + 273.15\right)^2 + \left(T_{gi} + 273.15\right)^2\right]\left[T_w + T_{gi} + 546\right] \qquad (8)$$

The effective emittance between water mass and glass cover ( ) is defined by the emissivity of water and glass cover:

$$\varepsilon_{eff} = \left(\frac{1}{\varepsilon_w} + \frac{1}{\varepsilon_g} - 1\right)^{-1} \qquad (9)$$

Many relations have been proposed to calculate and , namely Dunkle's model [25], Chen et al.'s model [26], Clark's model [27].

Dunkle estimated the value of using the following relation:

$$h_{c,w-gi} = 0.884 \times \left(\Delta T'\right)^{\frac{1}{3}} \qquad (10)$$

Where:

$$\Delta T' = \left[\left(T_w - T_{gi}\right) + \frac{\left(P_w - P_{gi}\right)\left(T_w + 273.15\right)}{268.9 \times 10^3 - P_w}\right] \qquad (11)$$

The saturation vapor pressures at water temperature and the glass cover inner surface temperature can be calculated from the below relations:

$$P_w = \exp\left[25.317 - \left(\frac{5144}{T_w + 273.15}\right)\right] \qquad (12)$$

$$P_{gi} = \exp\left[25.317 - \left(\frac{5144}{T_{gi} + 273.15}\right)\right] \qquad (13)$$

Moreover, Dunkle[25] used the following relation to calculate :

$$h_{e,w-g} = 0.0163 \times h_{c,w-g}\left[\frac{P_w - P_{gi}}{T_w - T_{gi}}\right] \qquad (14)$$

Chen et al. proposed the following relation to calculate :

$$h_{c,w-g} = 0.2Ra^{0.26}\frac{K_f}{d_f} \qquad (15)$$

To calculate Rayleigh number (Ra), the following relation can be used:

$$Ra = \frac{g\beta\left(T_w - T_{gi}\right)D^3}{\alpha v} \qquad (16)$$

In the concerned still, specific length (D) was considered equal to the diameter of the basin.

Clark proposed a model identical to Dunkle's model and developed the following corrected relation to calculate the rate of evaporative heat transfer:

$$q_{e,w-g} = \left(\frac{0.016273}{2}\right)h_{c,w-g}\left(P_w - P_{gi}\right) \qquad (17)$$

### 3.3. Heat balance equation for the water mass

$$\left(1-\alpha_g\right)\left(1-\rho_g\right)\left(1-\rho_w\right)\alpha_w G + h_{wb}\left(T_b - T_w\right) = h_{t,w-gi}\left(T_w - T_{gi}\right) \qquad (18)$$

The convective heat transfer coefficient between the basin liner and the water mass ( ) can be obtained by [28]:

$$h_{wb} = 0.54\frac{K_w Ra^{\frac{1}{4}}}{D} \qquad (19)$$

### 3.4. Heat balance equation for the basin and the insulation

$$\alpha_b\left(1-\alpha_g\right)\left(1-\rho_g\right)\left(1-\rho_w\right)\left(1-\alpha_w\right)G = h_{wb}\left(T_b - T_w\right) + h_b\left(T_b - T_a\right) \qquad (20)$$

The heat transfer coefficient between basin liner and ambient ( ) can be obtained by the following relation:

$$h_b = \left[\frac{L_{ins}}{K_{ins}} + \frac{1}{h_{loss}}\right] \qquad (21)$$

The overall heat loss coefficient from the insulation outer surface to ambient air ( ) can be calculated by the following relation [29]:

$$h_{loss} = 5.7 + 3.8V \qquad (22)$$

### 3.5. Distillate production and efficiency

The rate of distillate production (in ) can be obtained by the following relation:

$$m_w = \frac{h_{e,w-gi} \times A \times \left(T_w - T_{gi}\right)}{h_{fg}} \times 3600 \times 10^3 \qquad (23)$$

Furthermore, the instantaneous efficiency of the solar still is calculated by:

$$\eta_f = \frac{m_w \times h_{fg}}{A \times G} \qquad (24)$$

The physical properties assumed in the mathematical modeling are listed in Table 1.
Table1.Physical properties assumed in mathematical modeling [30-31].

$$h_{fg} = 2.506 \times 10^6 - 2.369 \times 10^3 T + 0.2678 T^2 - 8.103 \times 10^{-3}T^3 - 2.079 \times 10^{-5}T^4$$

$$\beta = \left(0.3 + 0.116T - 0.0004T^2\right) \times 10^{-4}$$

$$\nu = \left(\frac{1}{0.5155 + 0.0192T} - 0.12\right) \times 10^{-6}$$

$$K_f = 0.557 + 0.002198T - 0.0000057&T^2$$

## IV.    RESULTS AND DISCUSSION

The hourly variations of solar irradiance, ambient temperature, and wind speed that were measured during three days of testing are depicted in Figs. 3, 4, and 5, respectively. As expected, the profiles of solar radiation on the still had identical trends during three days of testing, i.e. they increased to their maximum values form the morning hours to the middle of the day and decreased in the afternoon. As can be observed in Fig .3, the values of solar radiation range between 130 and 910 w/m$^2$. Furthermore, due to the increase in the solar radiation in morning hours and its decrease in afternoon hours, the ambienttemperature increased to its maximum value from morning hours to the middle of the day and then showed a descending trend (see Fig. 4). The ambient temperature ranged from 22 to 40℃ in the testing days. Moreover, based on Fig. 5, the wind speed ranged between 1 and 3m/s during the testing days.
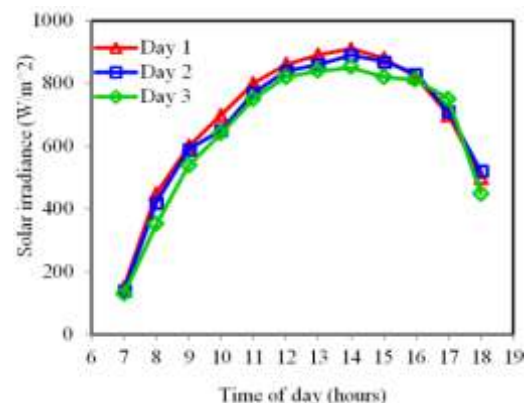


**Fig. 1.** The hourly variation of solar irradiance during the three days of testing the solar still.
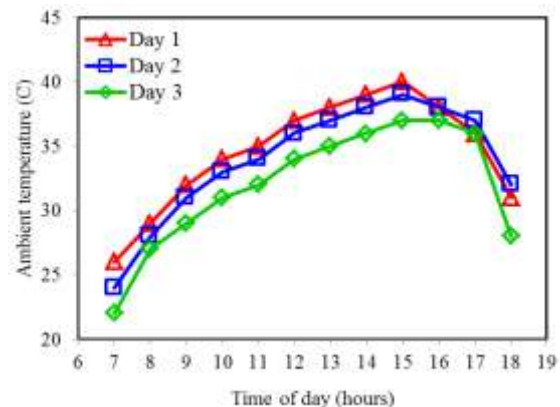


**Fig. 2.** The hourly variation of ambient temperature during the three days of testing the solar still.

The variations of solar still productivity during three days of testing and the predicted values by the modeling are shown in Figs. 6, 7, and 8. Also, as an example, Fig. 9 illustrates the accumulated solar productivity as a function of daytime for the third day of testing.

As can be observed in these figures, the solar still productivity followed a trend similar to the solar irradiance and reached its maximum value in the middle of the day. The solar productivity ranged between 5 and 390 ml/h (this maximum value was met at 15:00 on the first day of testing). The accumulated solar productivity ranged between 2720 ml for the third day of testing and 3175 ml for the first day of testing. This can be justified by the slightly higher value of solar irradiance on the first day (Fig. 3) and higher mean wind speed in this day (Fig. 5) since solar radiation is the most effective factor in the productivity of a solar still, i.e. higher solar radiation leads to significant enhancement of the solar still productivity [32]. Also, an increase in wind speed causes a decrease in temperature of the glass cover and, in turn, the temperature difference between the water and the glass cover is augmented which leads to the improvement of the natural circulation of air mass inside the still, yielding the enlargement of evaporative and convective heat transfer and productivity is escalated in the end [33-35].
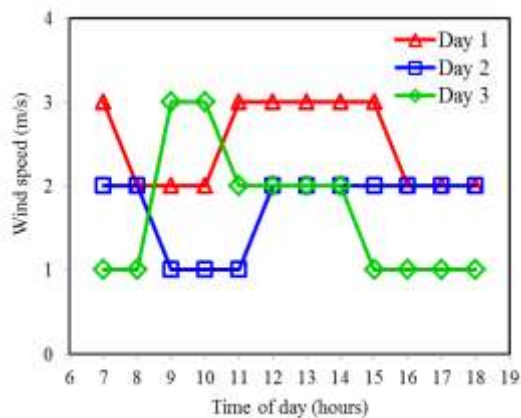


**Fig. 3.** The hourly variation of wind speed during the three days of testing the solar still.

Comparing the experimental results with the results obtained by the modeling, Clarke's model was found to provide closer results to the experimental data since Dunkle's and Chen's modelsnot only do assume evaporation surface (water surface) and condensation surface (glass cover surface) as parallel but also disregard the gap between them, which is not a valid assumption for the investigated experimental setup. Therefore the results obtained by Clarke's model considering the magnitude the distance between evaporation and condensation surfaces are more consistent with the experimental results. On the other hand, since Clarke's model is valid for the operating temperature beyond 50℃, its obtained results agree with the experimental data more accurately around the middle of the day when the solar radiation increases and the still more approaches the steady-state condition over time.

Fig. 10 shows the variation of the instantaneous efficiency of the still designed in this paper in comparison to similar stills proposed by other authors.As can be seen in Fig. 10, posing some slight variations in the glass cover inclination to approach the latitude of the test site along with the basin shape change from cone to low-height cylinder, the instantaneous efficiency significantly increased at least 5%.
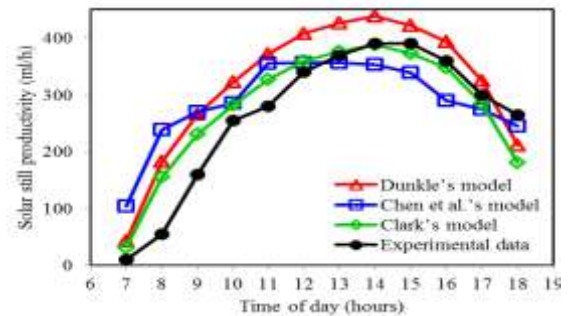


**Fig. 4.** The variation of solar still productivity during the first day of testing
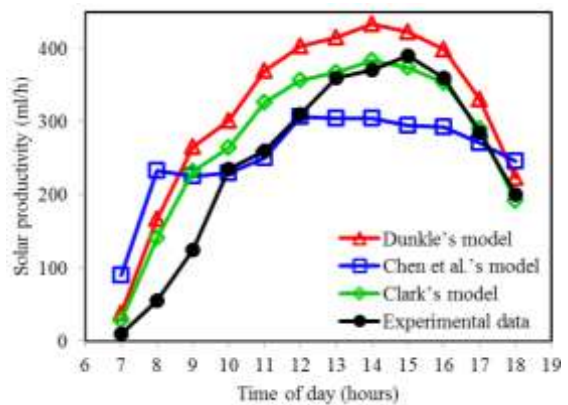


**Fig.7.** The variation of solar still productivity during the second day of testing
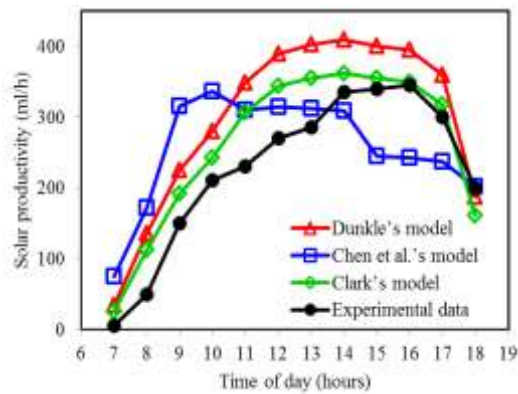
**Figure 8.** The variation of solar still productivity.



**Fig. 9**. The accumulated solar productivity during the third day of testing.

This is attributed to the fact that the annual productivity of solar stills reached its maximum value when the glass cover inclination equals the latitude of the test site [36].In addition to the decrease in the declination angle, the distance between the basin water and glass cover was dramatically reduced. Therefore, as presented by Al-Hussaini et al. [37], due to the volume reduction of non-condensable gas such as air (acting as a thermal barrier to the heat transfer), the efficiency of solar still is augmented. On the other hand, it has been illustrated that the efficiency of a solar still is in reverse proportion to the water depth in the basin [38-44]. Therefore, in the design proposed in this paper, the efficiency of the still was enhanced as much as possible by changing the shape of basin from cone to a low-height cylinder.

       Fig. 11 shows the variation of the instantaneous efficiency obtained from Clarck's model versus the variation of the glass cover thickness by mathematical modeling. As can be observed, the instantaneous efficiency diminishes by increasing the glass cover thickness since the heat transfer is improved and, in turn, the water vapor condensation rate is augmented [45]. Although the instantaneous efficiency increase due to the reduction in the glass cover thickness was insignificant (about 1%), reducing the glass cover thickness can diminish the final construction cost and ultimate weight of the still.
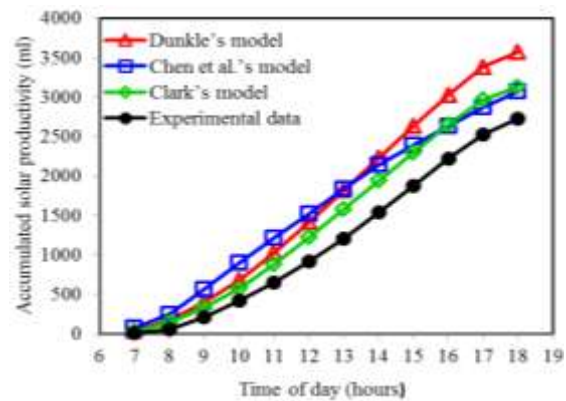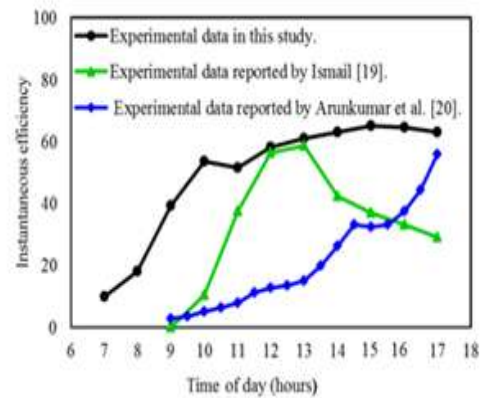


**Fig. 10**. Variations of instantaneous efficiency

       Fig. 12 and 13 depict the effects of insulation thickness and material on the instantaneous efficiency. As can be observed, increasing the insulation thickness to 15cm and decreasing the thermal conductivity to $0.1\,W/mK$, the instantaneous efficiency can reach 60% which is a substantially considerable value.
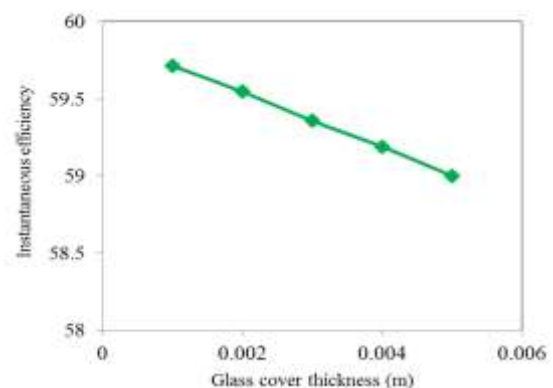


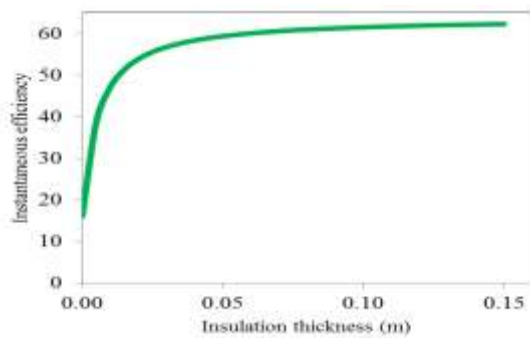**Fig. 11.** Effect of glass cover thickness on instantaneous efficiency

**Fig. 12.** Effect of insulation thickness on instantaneous efficiency
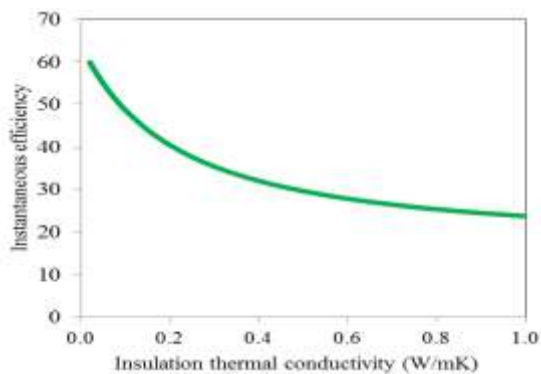


**Fig. 13.** Effect of insulation thermal conductivity on instantaneous efficiency

## V.    CONCLUSION

In the present study, a hemispherical solar still was built, experimentally investigated, and also modeled. It was intended in the fabrication of the still to increase the absorption of solar radiation and efficiency by geometric changes relative to similar stills. Examining the experimental and modeling results, Clark's model was found to provide a highly proper prediction of the system behavior. Furthermore, a decrease in glass cover thickness, an increase in insulation thickness, and a reduction in insulation thermal conductivity led to the improvement of efficiency.

## REFERENCES

[1]. Hidouri K, Slama RB, Gabsi S. (2010).**Hybrid Solar Still by Heat Pump Compression**. Desalination, 250, 444–449.

[2]. Bassam A. (2003). **Effect of Water Emissivity on Solar Still Efficiency**. International Journal of Sustainable Energy, 23(2), 13–19.

[3]. Delyannis E. (2003).**HistoricBackground of Desalination and Renewable Energies**. Solar Energy, 75(5), 357–366.

[4]. Siddiqqui M T, Jain A. (2015). **Analysis of Solar Still with Reflector**. International Journal for Technological Research in Engineering, 2(7), 1211–1216.

[5]. Malik MAS, Tiwari GN, Kumar A, Sodha MS. (1982). **Solar Distillation: a Practical Study of a Wide Range of Stills and Optimum Design, Construction and Performance**. New York: Pergamon Press.

[6]. Dhiman NK. (1988). **Transient Analysis of aSpherical Solar Still**. Desalination, 69, 47–55.

[7]. Haddad Z, Boukerzaza N. (2008). **Coupling Of a Spherical Solar Still witha Collector**. Journal of Engineering and Applied Sciences, 3(4), 317–321.

[8]. Rubio-Cerda E, Porta-Ga´ndara M A, Ferna´ndez-Zayas J L. (2002).**Thermal Performance of the Condensing Covers in a Triangular Solar Still**. Renewable Energy, 27,301–308.

[9]. Fath H ES, El-Samanoudy M, Fahmy K, Hassabou A. (2003). **Thermal-Economic Analysis and Comparison between Pyramid-Shaped and Single-Slope Solar Still Configurations**. Desalination, 159, 69–79.

[10]. Kianifar A, Heris S Z, Mahian O. (2012). **Exergy and Economic Analysis of a Pyramid-Shaped Solar Water Purification System: Active and Passive Cases**. Energy, 38, 31–36.

[11]. Ahsan A, Imteaz M, Thomas U A, Azmi M, Rahman A, Nikdaud N N. (2014). **Parameters Affecting the Performance of a Low Cost Solar Still**. Applied Energy, 114, 924–930.

[12]. Jamal W, Siddiqui M A. (2012). **Effect of Water Depth and Still Orientation on Productivity for Passive Solar Distillation**. International Journal of Engineering Research and Applications, 2(2), 1659–1665.

[13]. Arunkumar T, Jayaprakash R, Prakash A, Suneesh P U, Karthik M, Kumar S. (2010). **Study of Thermo Physical Properties and an Improvement in Production of Distillate Yield in Pyramid Solar Still with Boosting Mirror**. Indian Journal of Science and Technology, 3(8), 879–884.

[14]. Rahbar N, Asadi A, Fotouhi-Bafghi E. (2018). **Performance Evaluation of Two Solar Stills of Different Geometries: Tubular Versus Triangular: Experimental Study, Numerical Simulation, and Second Law Analysis**. Desalination, 443, 44–55.

[15]. Xie G, Sun L, Yan T, Tang J, Bao J, Du M. (2018). **Model Development and Experimental Verification for Tubular Solar Still Operating Under Vacuum Condition**. Energy, 157, 115–130.

[16]. Kabeel A E, Sharshir S W, Abdelaziz J B, Halim M A, Swidan. (2019). **Improving Performance Of Tubular Solar Still By Controlling The Water Depth And Cover Cooling**. Journal of Cleaner Production, 233, 848–856.

[17]. Rahbar N, Esfahani J A, Fotouhi-Bafghi E. (2015). **Estimation of Convective Heat Transfer Coefficient and Water-Productivity in a Tubular Solar Still – CFD Simulation and Theoretical Analysis**. Solar Energy, 113, 313–323.

[18]. Ahsan A, Imteaz M, Rahman A, Yusuf B, Fukuhara T. (2012). **Design, Fabrication and Performance Analysis of an Improved Solar Still**. Desalination, 292, 105–112.

[19]. Ismail B I, (2009). **Design and Performance of a Transportable Hemispherical Solar Still**. Renewable Energy, 34, 145–150.

[20]. Arunkumar T, Jayaprakash R, Denkenberger D, Ahsan A, Okundamiya M S, Kumar S, Tanaka H, Aybar H S. (2012). **An Experimental Study on a Hemispherical Solar Still**. Desalination, 286, 342–348.

[21]. Panchal H N, Shah P K. (2013). **Modeling and Verification Of Hemispherical Solar Still Using ANSYS CFD**. International Journal of Energy and Environment, 4(3), 427–440.

[22]. Rahman M M, Öztop H F, Ahsan A, Kalam M A, Varol Y. (2012). **Double-Diffusive Natural Convection in a Triangular Solar Collector**. International Communications in Heat and Mass Transfer, 39, 264–269.

[23]. Watmuff J H, Charters W W S, Proctor D. (1977). **Solar and Wind Induced External Coefficients - Solar Collectors**. Revue Internationaled'Heliotechnique.

[24]. Sharma V B, Mullick S C. (1991). **Estimation of Heat-Transfer Coefficients, the Upward Heat Flow, and Evaporation in a Solar Still**. ASME Journal of Solar Engineering, 113, 36–41.

[25]. Dunkle R V. (1961).**Solar Water Distillation: The Roof Type Still and a Multiple Effect Diffusion Still and a Multi Effect Diffusion Still**.Internal Developments in Heat Transfer, A.S.M.E, Proceedings of International Heat Transfer, Vol.5, University of Colorado, (1961) 895–902.

[26]. Chen Z, Ge X, Sun X, bar L, Miao Y X. (1984).**Natural Convection Heat Transfer across Air Layers at Various Angles of Inclination**. Engineering Thermophysics, 211–220.

[27]. Clark J A, (1990). **The Steady-State Performance of a Solar Still**. Solar Energy, 44(1), 43–49.

[28]. Halima H B, Frikha N, Slama R B. (2014). **Numerical Investigation of a Simple Solar Still Coupled to a Compression Heat Pump**. Desalination, 337, 60–66.

[29]. Duffie J A, Beckman, W, A. (2013). **Solar Engineering of Thermal Processes**. John Wiley & Sons, New York.

[30]. Kofi P M E, Andoh H Y, Gbaha P, Toure S, Ado G. (2008). **Theoretical and Experimental Study of Solar Water Heater with Internal Exchanger Using Thermosiphon System**. Energy Conversion and Management, 49, 2279–2290.

[31]. International association for the properties of water and steam, Release on the IAPWS Formulation 1995 for the thermodynamic properties of ordinary water substance for general and scientific use, 1996.

[32]. SafwatNafey A, Abdelkader M, Abdelmotalip A, Mabrouk A A. (2000). **Parameters Affecting Solar Still Productivity**. Energy Conversion & Management, 41, 1797–1809.

[33]. El-Sebaii A A. (2000). **Effect of Wind Speed on Some Designs of Solar Stills**. Energy Conversion & Management, 41, 523–538.

[34]. Zurigat Y H, Abu-Arabi M K. (2004). **Modelling and Performance Analysis of a Regenerative Solar Desalination Unit**. Applied Thermal Engineering, 24, 1061–1072.

[35]. Dunkle RV. (1961).**Solar Water Distillation: The Roof Type Still and a Multiple Effect Diffusion still**. In: Proceedings of the international conference of heattransfer, University of Colorado,108, 895–902.

[36]. Singh H N, Tiwari G N. (2004). **Monthly Performance of Passive and Active Solar Stills for Different Indian Climatic Conditions**. Desalination, 168, 145–150.

[37]. Al-Hussain H, Smith I K. (1995). **Enhancing of Solar Still Productivity Using Vacuum Technology**.Energy Conversion and Management, 36 (11), 1047–1051.

[38]. Tripath R, Tiwari G N. (2005). **Effect of Water Depth on Internal Heat and Mass Transfer for Active Solar Distillation**. Desalination, 173. 187–200.

[39]. Tripath R, Tiwari G N. (2006). **Thermal Modeling of Passive and Active Solar Stills for Different Depths of Water by**

**Using the Concept of Solar Fraction**. Solar Energy, 80, 956–967.

[40]. Phadatare M K, Verma S K. (2007). **Influence of Water Depth on Internal Heat and Mass Transfer in a Plastic Solar Still**. Desalination, 217, 267–275.

[41]. Suneja S, Tiwari G N. (1999). **Effect of Water Depth on the Performance of an Inverted Absorber Double Basin Solar Still**. Energy Conversion & Management, 40, 1885–1897.

[42]. Akash B A, Mohsen M S, Nayfeh W. (2000). **Experimental Study of the Basin Type Solar Still under Local Climate Conditions**. Energy Conversion & Management, 41, 883–890.

[43]. Rajamanickam M R, Ragupathy A. (2012). **Influence of Water Depth on Internal Heat and Mass Transfer in a Double Slope Solar Still**. Energy Procedia, 14, 1701–1708.

[44]. Abdul-Wahab S A, Al-Hatmi Y Y. (2013). **Performance Evaluation of an Inverted Absorber Solar Still Integrated with a Refrigeration Cycle and an Inverted Absorber Solar Still**. Energy for Sustainable Development, 17, 642–648.

[45]. Ghoneyem A, Ileri A. (1997). **Software to Analyze Solar Stills and an Experimental Study on the Effects of the Cover**.Desalination, 114, 37–44.

[46]. Effect Diffusion Still". Proc. Intl. Heat Transfer, ASME, Part V, University of Colorado, USA, pp. 895-902, 1961

[47]. Dunkle, R.V. "Solar Water Distillation: The Roof Type Still And A Multiple Effect Diffusion Still". Proc. Intl. Heat Transfer, ASME, Part V, University of Colorado, USA, pp. 895-902, 1961